第 43 卷 第 9 期/2023 年 5 月/光学学报 研究论文

光学学报

新型窗帘式WO_3基电致变色器件设计与制备

陈国新[1]，陈浩元[1]，张志勇[1]，张臣臣[1]，唐秀凤[1,2*]，詹云凤[1,2**]，罗坚义[1,2***]

[1]五邑大学应用物理与材料学院，广东 江门 529020；

[2]五邑大学柔性传感材料与器件研究开发中心，广东 江门 529020

摘要 采用磁控溅射法制备氧化钨(WO_3)，基于电流驱动模型设计制备无需对电极层的新型窗帘式电致变色器件，并对器件的边框、WO_3薄膜的最佳厚度和离子储存区尺寸进行了系统优化。结果表明，制备得到的WO_3薄膜在550 nm波长处的调制率高达78%，1000圈循环伏安曲线测试后电荷储量衰减率仅为3.5%；设计的窗帘式器件显色区域高度可控，且消除了对电极对器件性能的影响。该研究为电致变色器件结构创新提供了新思路。

关键词 薄膜；氧化钨；电致变色；窗帘式；结构简化

中图分类号 O484 **文献标志码** A **DOI**：10.3788/AOS221809

1 引 言

电致变色(EC)是指材料的反射率、透过率、吸收率等光学特性在外加电场的作用下表现出可逆、稳定变化的现象[1]。由于节能环保、智能可控等优点，电致变色技术在调光智能窗户[2]、防眩目后视镜[3]、电子报纸和双稳态显示[4-5]、突触晶体管[6]及各种光电子器件[7-8]中应用广泛，一直以来都是各国学者争相研究的热点[9-11]。人们做了大量的研究工作，使电致变色器件更加多彩[12-13]、性能更加优异[14-15]、功能更加集成[16-17]。其中氧化钨(WO_3)薄膜作为应用最广泛的无机电致变色材料，其变色机理相对清晰、制备工艺更为成熟，且自身具备显色效率高、对比度高、记忆时间长、化学稳定性好等优点[18-19]。因此，目前WO_3基电致变色器件产业化最为成熟。

一个传统的WO_3基电致变色器件至少包含5层功能层，即上透明电极氧化铟锡(ITO)层、对电极层、电解质层、WO_3变色层和下透明电极ITO层[20]，其中对电极层需要在离子储量及颜色上与WO_3变色层严格匹配，且对电极的存在会降低器件在透明态时的透过率。更为重要的是，常见的对电极层，如NiO、TiO_2薄膜等，存在易脱落、易分解及与WO_3电化学性能不匹配等问题，这大大加速了电致变色器件的失效过程[21-22]。然而，相较于对WO_3变色层的研究[23-25]，人们对电致变色器件结构优化的关注度较少。Fang等[26]通过直接将多功能离子水凝胶堆积在WO_3薄膜上，制备得到了只有三层功能层的电致变色书写笔，实现了较好的变色性能。Pan等[27]使用海带褐藻和水母，同时与作为凝胶电解质的电致变色紫精双(3-羟丙基)二溴紫精和作为电子介质的1,1′-二茂铁二甲酸和1,1′-二茂铁二甲醇混合，制备了一体化的生物型电致变色器件。Howard等[28]通过混合共轭电致变色聚合物，实现了底部导电层的去除，简化了电致变色器件结构。上述研究工作均证明了器件结构优化的可行性。然而，相关研究结果却难以解决现有WO_3基电致变色器件中的对电极问题。因此本文借助电流驱动模型[29]，通过系统设计去除对电极层，制备WO_3基电致变色器件，这样可在简化结构的同时实现器件的窗帘式变色模式，打破了电致变色器件现在仅有的整体变色方式。

2 实 验

2.1 窗帘式智能窗制备

本实验采用磁控溅射法制备WO_3薄膜，使用的镀膜设备为高真空磁控溅射仪(北京泰科诺JCP500型)，以ITO透明导电玻璃(ITO厚度约为110 nm，电阻为8 Ω/sq)为衬底，以金属钨(纯度为99.99%)为靶材，工作气压为1.4 Pa，氩气流量为12 sccm (1 sccm=1 m^3/min)，氧气流量为4.8 sccm，溅射功率为80 W，基底温度为200 ℃。实验利用不同的溅射时间获得不同厚度的WO_3薄膜。器件使用浓度为1 mol/L的$LiClO_4$-PC电解质，由高氯酸锂($LiClO_4$)和碳酸丙烯酯(PC)以1∶3的质量比混合搅拌制得。最后用UV胶

收稿日期：2022-10-11；**修回日期**：2022-11-03；**录用日期**：2022-11-25；**网络首发日期**：2022-12-05

基金项目：广东省基础与应用基础研究基金联合基金青年项目(2019A1515110778)、2022年广东大学生科技创新培养专项资金(“攀登计划”专项基金)(pdjh2022a0522，pdjh2022a0524)

通信作者：*tbrenda@sina.com；**zhanyf6@163.com；***luojiany@mail3.sysu.edu.cn

将ITO透明导电玻璃、电解质和WO_3薄膜封装得到WO_3基窗帘式电致变色器件。

为了与窗帘式器件进行对比，选用TiO_2薄膜作为对电极层，与WO_3薄膜组装得到传统结构的电致变色器件。其中TiO_2对电极同样以上述ITO透明导电玻璃为衬底，采用溶胶-凝胶提拉法制备；原料为钛酸四丁酯、冰乙酸、无水乙醇和去离子水；先将钛酸四丁酯和无水乙醇按3∶8的体积比混合，将冰乙酸、无水乙醇和去离子水按15∶80∶3的体积比混合，然后将醋酸溶液缓慢滴入钛酸四丁酯溶液中，得到其溶胶-凝胶A；再将ITO透明导电玻璃放入A中浸泡10 s，然后以2 mm/min的速度提拉，重复提拉3次，最后将其放入马弗炉内在450 ℃退火2 h，获得厚度约为80 nm的TiO_2薄膜。

2.2 测试与表征

WO_3薄膜的基本表征：采用场发射电子扫描显微镜(Sigma 500 Zeiss)表征薄膜的表面形貌，电子束加速电压为10 kV，测试前需要对薄膜进行喷金处理；采用X射线衍射仪(X' Pert Philips)测试薄膜的晶体结构，以Cu靶Kα射线作为X射线源，扫描范围为10°～80°，步幅为0.02°；利用ESCALAB 250Xi(Thermo Fisher Scientific)型X射线光电子能谱仪进行XPS测试。

WO_3薄膜电致变色性能测试：使用电化学工作站(上海辰华CHI760E)进行循环伏安曲线测试(CV)，其中以WO_3薄膜为工作电极、Pt为对电极、Ag/AgCl为参比电极、浓度为1 mol/L的$LiClO_4$-PC为电解质溶液，扫描电压为－0.8～0.8 V，扫描速度为100 mV/s。采用紫外-可见光分光光度计(日立F-4600)测量薄膜透过率。

器件的循环寿命和响应时间测试方法如下：1)在垂直方向施加3 V电压，WO_3薄膜整体着色，此时薄膜在550 nm波长处的透过率定义为器件的初始透过率；2)施加水平电压，保持工作电流为0.2 A，将锂离子驱赶到一端直至薄膜着色状态不再变化，将此过程所用时间定义为器件响应时间；3)撤掉水平电压，锂离子自由扩散，待薄膜内各处透过率差小于1%时，视为薄膜此时再次呈均匀着色态，将此过程所用时间定义为器件恢复时间。步骤1)～3)称为器件的一个工作循环。重复步骤1)～3)，直到薄膜的着色态透过率高于60%，循环次数被定义为器件单次注入后的循环寿命。

3 结果与讨论

3.1 高性能WO_3薄膜制备

对沉积在ITO玻璃衬底上厚度为800 nm的WO_3薄膜进行了X射线衍射(XRD)、X射线光电子能谱(XPS)和扫描电子显微镜(SEM)表征。由图1(a)可以看出，WO_3薄膜的XRD特征峰的半峰全宽很宽，表明薄膜为非晶态，与文献报道一致[29]。在电致变色应用中，非晶态薄膜结构更为疏松，缺陷和孔洞较多，有利于离子的注入与抽出，因此非晶态WO_3薄膜比晶态薄膜变色性能更加优异[30]。图1(b)中XPS谱图表明，所制薄膜中的W元素只有一种价态，为＋6价，即制得的薄膜为WO_3薄膜[31]，SEM图片显示薄膜表面平整，WO_3颗粒均匀且薄膜存在较多孔隙，如图1(c)所示。

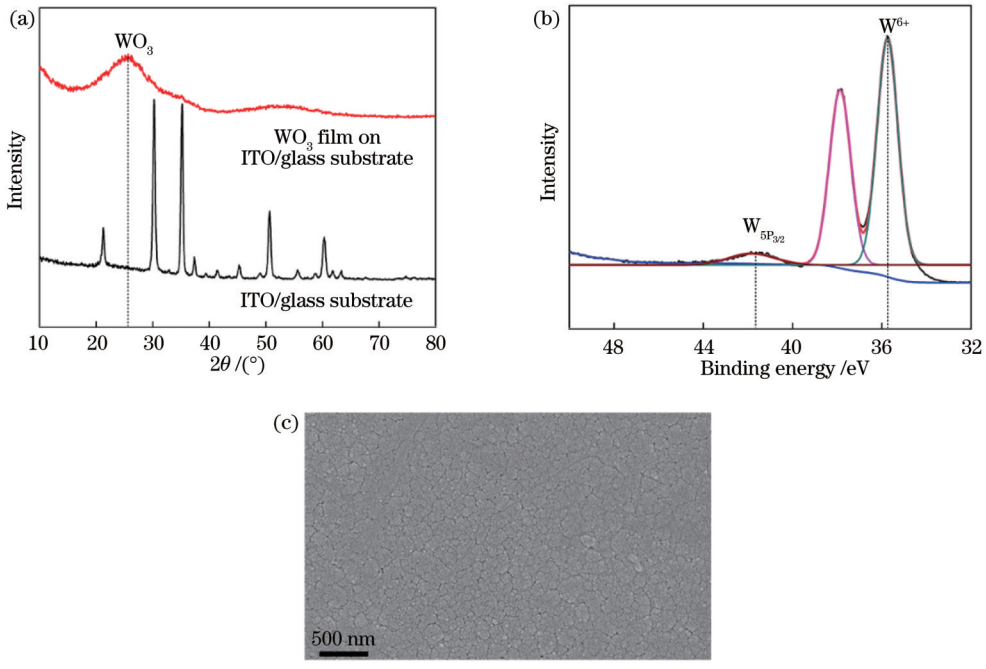

图1 沉积在ITO玻璃衬底上的800 nm厚WO_3薄膜。(a) XRD图；(b) XPS；(c) SEM照片

Fig. 1 WO_3 film with thickness of 800 nm deposited on ITO glass substrate. (a) XRD pattern; (b) XPS; (c) SEM photo

衡量薄膜电致变色性能的参数有光学调制率、循环寿命、响应时间等。大的光学调制率意味着材料具有大的透过率调控范围。图 2(a)为制得的 WO_3 薄膜在电压为 3 V、着色时间和褪色时间均为 1 min 的工作条件下，原始态、着色态和褪色态的透过率曲线。可以看出 WO_3 薄膜在 550 nm 波长的原始态透过率为 72.5%，着色态透过率为 5%，褪色态透过率为 83%，薄膜的调制率高达 78%。另外，电致变色薄膜的实用性很大程度上取决于其循环稳定性。图 2(b)是制得 WO_3 薄膜的 CV 循环曲线，测试用 WO_3 薄膜的面积为 1 cm^2。测试过程中，WO_3 薄膜先由透明逐渐变成深蓝（电压范围为 −0.8～0 V），再由深蓝褪色为透明（电压范围为 0～0.8 V），对应于锂离子的注入和抽出过程。根据公式 $Q=\int(JdV)/S$[31]（其中 Q 为总电荷量，J 为电流密度，V 为电压，S 为薄膜的面积），可计算得到 WO_3 薄膜第 1 圈时的电荷储存量约为 28.8 mC/cm^2，经过 1000 圈 CV 循环后电荷储存量为 27.8 mC/cm^2，衰减率仅为 3.5%，薄膜表现出优异的循环稳定性。本文制得 WO_3 薄膜的光学调制率及循环性能远优于其他报道[32-35]。

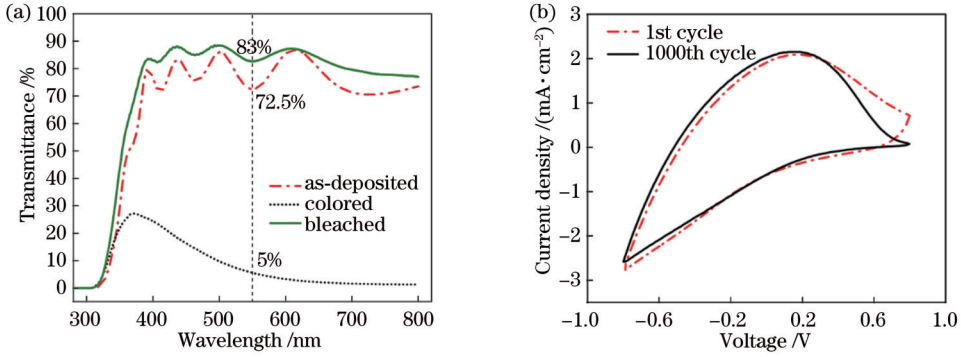

图 2　WO_3 薄膜电致变色性能。(a)透过率曲线；(b) CV 循环曲线图

Fig. 2　Electrochromic properties of WO_3 film. (a) Transmittance curves; (b) CV cyclic curves

3.2　窗帘式 WO_3 基电致变色器件设计

垂直加压使锂离子注入 WO_3 薄膜后，在 WO_3 薄膜底部的 ITO 电极中通水平方向的电流可以使注入到薄膜中的锂离子发生水平可控运动（即电流驱动模型），从而实现 WO_3 薄膜的窗帘式变色模式，即无需通过反向加压抽出锂离子便可实现薄膜褪色[29]。因此，本文基于电流驱动模型设计新型窗帘式电致变色器件，如图 3 所示。图 3(a)对比了本文设计结构与传统电致变色器件的结构，可以看出，本文设计的窗帘式器件去掉了对电极功能层，不仅能够消除对电极层对器件透过率和循环稳定性的影响，同时可以实现器件结构和制备工艺的简化。该窗帘式智能窗的工作方式如图 3(b)所示。在垂直方向上施加电压对 WO_3 薄膜进行着色，通过在 WO_3 底部 ITO 导电层中通 0.2 A 的工作电流将注入的 Li^+ 驱赶到薄膜一端，薄膜一端褪色，另一端着色加深；撤掉电流后，Li^+ 扩散，器件变色恢复均匀。其中：工作过程中 Li^+ 聚集的薄膜区域称为离子储存区；离子抽出的区域称为窗户区即工作区域，用于遮光

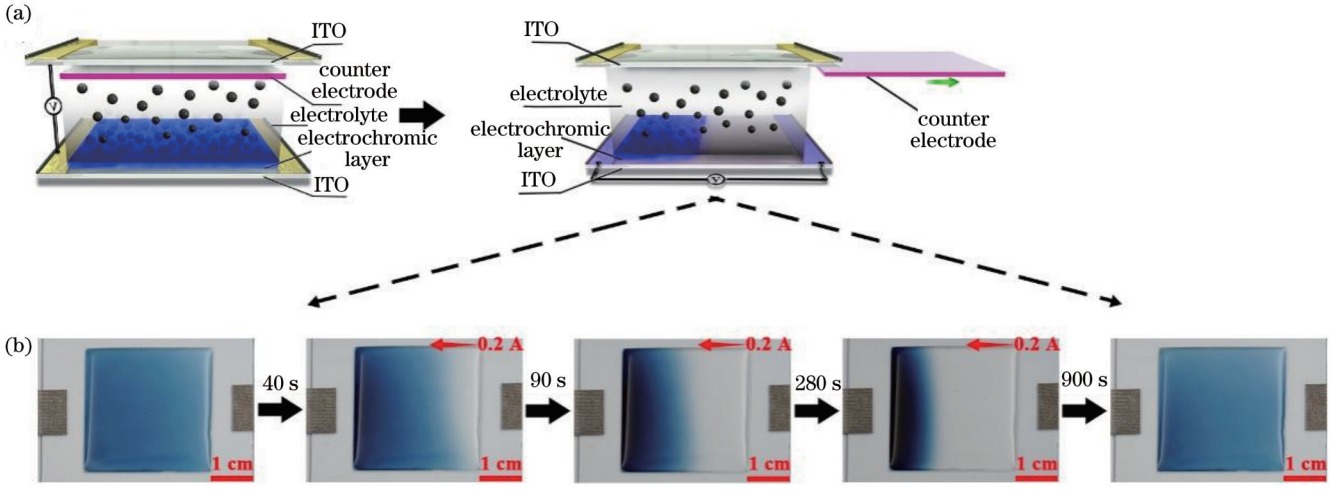

图 3　窗帘式电致变色器件设计。(a)传统电致变色器件结构与窗帘式电致变色器件对比图；(b)窗帘式电致变色器件工作过程照片

Fig. 3　Design of curtain-like electrochromic devices. (a) Structure comparison between traditional electrochromic device and curtain-like color-changing device; (b) photos of working process of curtain-like electrochromic device

和透光。因此，本文设计的窗帘式电致变色器件可以在不同方向的工作电流控制下实现着色和褪色切换。

为了便于工作区域的边框设计，在 WO_3 薄膜中采用激光切割出一条微米级隔痕，将薄膜人为分隔为离子储存区与窗户工作区，储存区和窗户区长度比例设置为 1∶2，如图 4(a)所示。图 4(b)的测试结果表明，存在隔痕的器件褪色更快，工作过程中存在隔痕的器件窗户区褪色时间为 155 s，透过率从 40% 上升到 83.8%，没有隔痕器件的窗户区褪色时间为 200 s，透过率从 40% 上升到 78%[数据采集点为图 4(a)中点 M]。撤掉工作电流后，隔痕的存在也可以加速窗户区域的恢复着色过程[数据采集点为图 4(a)中点 R]。且有隔痕的器件窗户区调制率比无隔痕器件高 5.8%，透明态时更为透明，着色态时透过率也更低。由器件工作照片也可以看出有隔痕设计的器件工作时离子存储区和工作区边界更加清晰，有利于边框的确定，器件的美观性也更好，这可能是由薄膜隔痕处的边界聚集效应导致的。

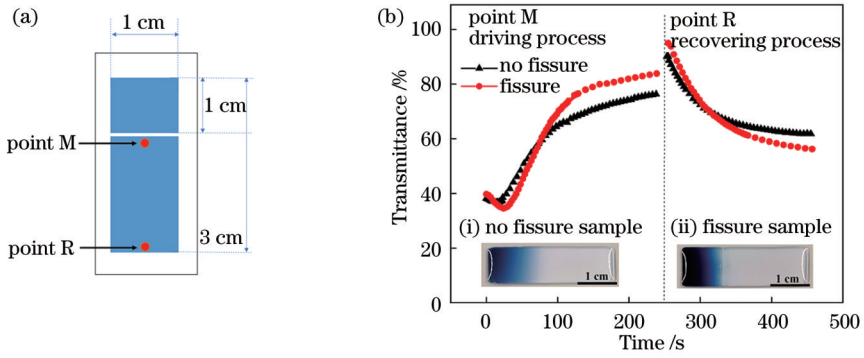

图 4　窗帘式 WO_3 基电致变色器件边框设计。(a)在离子存储区和工作区之间人为制造隔痕作为边框时的器件设计模型图；(b)有、无隔痕边框设计的器件工作过程对比，其中插图为器件工作照片

Fig. 4　Bezel design of curtain-like WO_3-based electrochromic device. (a) Illustration of design with man-made fissure between storage area and working area of ions; (b) comparison between working processes of devices with and without fissure design (insets are working photos of two devices)

薄膜厚度对器件性能的影响显著，如图 5 所示。本文制备了厚度分别为 400 nm、800 nm、1200 nm、1600 nm、2000 nm 的 WO_3 薄膜，测试薄膜厚度对器件响应时间、恢复时间和循环寿命的影响。结果表明，薄膜厚度对器件响应时间的影响较小，其中 400 nm 的 WO_3 薄膜的着色时间最快为 129.5 s，800 nm WO_3 薄膜的着色时间为 130.7 s。但是薄膜厚度对器件恢复时间和循环寿命的影响显著，其中器件的恢复时间随着薄膜厚度的增大呈现先缩短后延长最后趋于平缓的变化过程；而器件的循环寿命则随着薄膜厚度的增大先延长随后急剧单调缩短。特别的是，800 nm 的 WO_3 薄膜同时为恢复时间最短处和循环寿命最长处，最短恢复时间为 234.7 s，循环寿命最长为 32 圈。这是由于：薄膜厚度过小时，器件的光学调制范围和离子储存能力受到限制；薄膜厚度过大则导致 WO_3 薄膜附着力小，在器件工作过程中离子运动引入的薄膜应力使薄膜容易脱落失效。

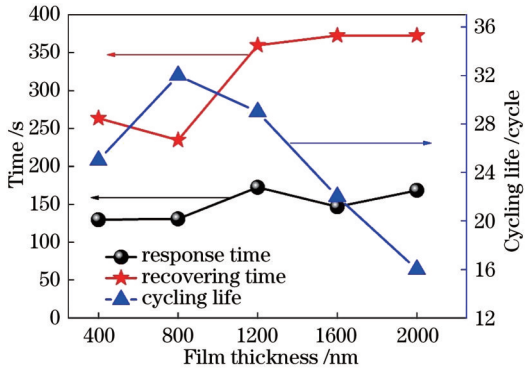

图 5　WO_3 薄膜厚度对器件响应时间、恢复时间和循环寿命的影响

Fig. 5　Effect of WO_3 film thickness on response time, recovery time, and cyclic life

为了延长窗帘式器件的循环寿命，本文对器件的离子储存区尺寸进行了三种设计，分别为 1 cm×1 cm、1 cm×2 cm、1 cm×3 cm，分析储存区尺寸对器件性能的影响，如图 6 和表 1 所示。实验数据表明，随着离子储存区面积的增大，器件的循环寿命延长。相较于储存区面积为 1 cm×1 cm 时器件循环 32 次后便出现脱落失效的情况，当储存区尺寸为 1 cm×2 cm 且与工作区域相同时，器件寿命显著延长，循环 100 次仍然完好。然而，器件的变色响应时间和恢复时间会随着储存区面积的增大而延长。因此，离子储存区面积为 1 cm×2 cm 且与窗户区面积一致时，器件性能最佳。

3.3　窗帘式 WO_3 基电致变色器件制备

采用最佳设计参数，以高性能 WO_3 薄膜为变色功能层，制备得到窗帘式电致变色器件。如图 7(a)所示，在波长 550 nm 处，器件的透明态透过率为 76%，相比于传统结构器件(有对 TiO_2 电极层，如插图所示)的

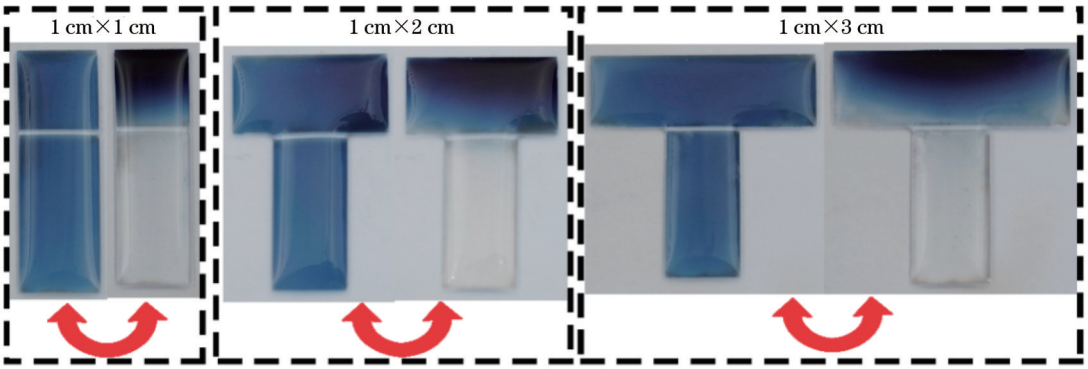

图 6　不同储存区尺寸的窗帘式 WO_3 基电致变色器件工作过程照片

Fig. 6　Working process photos of curtain-like WO_3-based electrochromic devices with different sizes of storage area

表 1　储存区尺寸对器件响应时间、恢复时间和循环寿命的影响

Table 1　Effect of storage area size on response time, recovery time, and cyclic life of device

Storage area / cm^2	Cycling life / cycle	Response time /min	Recovering time /min
1	32	2.2	3.9
2	⩾100	2.7	4.4
3	⩾100	3.0	5.2

67% 透明态透过率高出 9 个百分点。如图 7(b)所示，窗帘式器件显示出优异的记忆效应，放置 10 d 后，器件在波长 550 nm 处的着色态透过率从 20% 仅上升到 27.5%。高的透明态透过率意味着器件可以提供更为清晰的底部信息，优异的记忆效应可有效减少维持器件常关态低透过率的电量消耗，所以本文设计制备的窗帘式器件在信息加密、名画保护等领域有着极大的优势和广阔的应用前景。

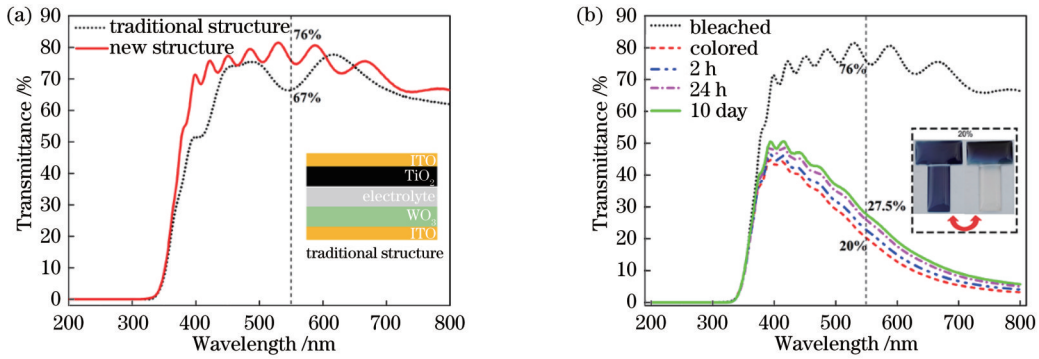

图 7　窗帘式 WO_3 基电致变色器件性能。(a)窗帘式器件与传统器件褪色态透过率对比，插图为传统器件结构示意图；(b)窗帘式器件记忆效应曲线，插图为器件着色和褪色态照片

Fig. 7　Performances of curtain-like WO_3-based electrochromic device. (a) Transmittance comparison between traditional device and curtain-like device (inset is structure illustration of traditional device); (b) memory effect of curtain-like device (insets are photos of device respectively in colored and bleached states)

4　结　　论

通过磁控溅射法制备了性能优异的 WO_3 薄膜，薄膜在 550 nm 波长的调制率高达 78%，1000 圈 CV 循环后电荷存储量衰减率仅为 3.5%。基于电流驱动模型设计无需对电极层的新型窗帘式电致变色器件，并对器件的边框、WO_3 薄膜的最佳厚度和离子储存区尺寸进行了系统设计。结果表明，在 WO_3 薄膜中人为设计隔痕能够同时缩短器件的响应时间和提高调制率，且有利于工作区域的边框设计；WO_3 薄膜厚度为 800 nm 时，器件的综合性能均为最佳；离子储存区域和工作区域面积相近时，器件的循环寿命能够得到保证。采用最佳设计参数制备的窗帘式 WO_3 基电致变色器件性能优异，在波长 550 nm 处器件的透明态透过率为 76%，比有 TiO_2 薄膜作对电极的传统器件高出 9 个百分点；在 20% 透过率下放置 10 d 后，器件透过率仅上升 7.5 个百分点，呈现出优异的记忆效应。这些特性使窗帘式器件在信息加密、名画保护等领域有着极大的应用优势。相比于传统结构，本文设计制备的窗帘式电致变色器件具有结构更为简单、显色区域高度可控等优点，对电致变色器件的结构创新具有重要指导意义。

参　考　文　献

[1]　Granqvist C G. Out of a niche[J]. Nature Materials, 2006, 5(2): 89-90.

[2] Jin Y, Zhou L, Liang J, et al. Electrochemically driven dynamic plasmonics[J]. Advanced Photonics, 2021, 3(4): 044002.

[3] Bange K, Gambke T. Electrochromic materials for optical switching devices[J]. Advanced Materials, 1990, 2(1): 10-16.

[4] Bach U, Corr D, Lupo D, et al. Nanomaterials-based electrochromics for paper-quality displays[J]. Advanced Materials, 2002, 14(11): 845-848.

[5] Zhang W R, Wang X J, Wang Y Y, et al. Bio-inspired ultra-high energy efficiency bistable electronic billboard and reader[J]. Nature Communications, 2019, 10: 1559.

[6] Yang C S, Shang D S, Liu N, et al. All-solid-state synaptic transistor with ultralow conductance for neuromorphic computing [J]. Advanced Functional Materials, 2018, 28(42): 1804170.

[7] Xiao L L, Lü Y, Lin J, et al. WO_3-based electrochromic distributed Bragg reflector: toward electrically tunable microcavity luminescent device[J]. Advanced Optical Materials, 2018, 6(1): 1700791.

[8] Qi C J, Chen G X, Huang T C, et al. Greatly simplified all-solid-state camera shielding device of mobile phone based on the shoulder-by-shoulder electrochromic technology[J]. ACS Applied Electronic Materials, 2021, 3(6): 2631-2637.

[9] 范宏伟, 李克睿, 侯成义, 等. 多功能电致变色器件: 从多器件到单器件集成[J]. 无机材料学报, 2021, 36(2): 115-127.
Fan H W, Li K R, Hou C Y, et al. Multi-functional electrochromic devices: integration strategies based on multiple and single devices[J]. Journal of Inorganic Materials, 2021, 36 (2): 115-127.

[10] Ling H, Wu J C, Su F Y, et al. Automatic light-adjusting electrochromic device powered by perovskite solar cell[J]. Nature Communications, 2021, 12: 1010.

[11] 钟晓岚, 刘雪晴, 刁训刚. 基于氧化钨和氧化镍的电致变色器件研究进展[J]. 无机材料学报, 2021, 36(2): 128-139.
Zhong X L, Liu X Q, Diao X G. Electrochromic devices based on tungsten oxide and nickel oxide: a review[J]. Journal of Inorganic Materials, 2021, 36(2): 128-139.

[12] Xu T, Walter E C, Agrawal A, et al. High-contrast and fast electrochromic switching enabled by plasmonics[J]. Nature Communications, 2016, 7: 10479.

[13] Zhang Q, Tsai C Y, Li L J, et al. Colorless-to-colorful switching electrochromic polyimides with very high contrast ratio [J]. Nature Communications, 2019, 10: 1239.

[14] Weng W, Higuchi T, Suzuki M, et al. A high-speed passive-matrix electrochromic display using a mesoporous TiO_2 electrode with vertical porosity[J]. Angewandte Chemie International Edition, 2010, 49(23): 3956-3959.

[15] Tian Y Y, Zhang W K, Cong S, et al. Unconventional aluminum ion intercalation/deintercalation for fast switching and highly stable electrochromism[J]. Advanced Functional Materials, 2015, 25(36): 5833-5839.

[16] 王星佺, 卞正兰. Pt-WO_3纳米氢敏薄膜的制备及传感特性研究[J]. 激光与光电子学进展, 2023, 60(7): 0731001.
Wang X Q, Bian Z L. Preparation of Pt-WO_3 nano-hydrogen sensitive film and research on its sensing properties[J]. Laser & Optoelectronics Progress, 2023, 60(7): 0731001.

[17] 李嘉丽, 洪婉玲, 赵春柳, 等. 基于阵列波导光栅的光纤法布里-珀罗干涉仪型多点氢气传感器[J]. 光学学报, 2021, 41(13): 1306013.
Li J L, Hong W L, Zhao C L, et al. Multi-point optical fiber hydrogen sensor with Fabry-Perot interferometers using arrayed waveguide grating[J]. Acta Optica Sinica, 2021, 41(13): 1306013.

[18] Granqvist C G. Electrochromics for smart windows: oxide-based thin films and devices[J]. Thin Solid Films, 2014, 564: 1-38.

[19] Zhao Q, Fang Y S, Qiao K, et al. Printing of WO_3/ITO nanocomposite electrochromic smart windows[J]. Solar Energy Materials and Solar Cells, 2019, 194: 95-102.

[20] Granqvist C G, Azens A, Heszler P, et al. Nanomaterials for benign indoor environments: electrochromics for "smart windows", sensors for air quality, and photo-catalysts for air cleaning[J]. Solar Energy Materials and Solar Cells, 2007, 91 (4): 355-365.

[21] Dong D M, Wang W W, Rougier A, et al. Life-cycling and uncovering cation-trapping evidence of a monolithic inorganic electrochromic device: glass/ITO/WO_3/$LiTaO_3$/NiO/ITO[J]. Nanoscale, 2018, 10(35): 16521-16530.

[22] Khalifa Z S. Electronic structure changes of TiO_2 thin films due to electrochromism[J]. Solar Energy Materials and Solar Cells, 2014, 124: 186-191.

[23] Yao Y J, Zhao Q, Wei W, et al. WO_3 quantum-dots electrochromism[J]. Nano Energy, 2020, 68: 104350.

[24] Wang W Q, Wang X L, Xia X H, et al. Enhanced electrochromic and energy storage performance in mesoporous WO_3 film and its application in a bi-functional smart window[J]. Nanoscale, 2018, 10(17): 8162-8169.

[25] Arvizu M A, Qu H Y, Cindemir U, et al. Electrochromic WO_3 thin films attain unprecedented durability by potentiostatic pretreatment[J]. Journal of Materials Chemistry A, 2019, 7(6): 2908-2918.

[26] Fang H J, Zheng P Y, Ma R, et al. Multifunctional hydrogel enables extremely simplified electrochromic devices for smart windows and ionic writing boards[J]. Materials Horizons, 2018, 5(5): 1000-1007.

[27] Pan M J, Zhao S, Ma L, et al. All-in-one electrochromic devices with biological tissues used as electronic components[J]. Solar Energy Materials and Solar Cells, 2019, 189: 27-32.

[28] Howard E L, Österholm A M, Shen D E, et al. Cost-effective, flexible, and colorful dynamic displays: removing underlying conducting layers from polymer-based electrochromic devices[J]. ACS Applied Materials & Interfaces, 2021, 13(14): 16732-16743.

[29] Tang X F, Chen G X, Mo Z P, et al. Controllable two-dimensional movement and redistribution of lithium ions in metal oxides[J]. Nature Communications, 2019, 10: 2888.

[30] Washizu E, Yamamoto A, Abe Y, et al. Optical and electrochromic properties of RF reactively sputtered WO_3 films [J]. Solid State Ionics, 2003, 165(1/2/3/4): 175-180.

[31] Wen R T, Granqvist C G, Niklasson G A. Eliminating degradation and uncovering ion-trapping dynamics in electrochromic WO_3 thin films[J]. Nature Materials, 2015, 14 (10): 996-1001.

[32] Chang C M, Chiang Y C, Cheng M H, et al. Fabrication of WO_3 electrochromic devices using electro-exploding wire techniques and spray coating[J]. Solar Energy Materials and Solar Cells, 2021, 223: 110960.

[33] 初文静, 林俊良, 郑友伟, 等. 聚合物前驱体法制备WO_3薄膜的电致变色性能[J]. 光学学报, 2018, 38(2):0216002.
Chu W J, Lin J L, Zheng Y W, et al. Electrochromic performance of WO_3 films prepared by polymeric precursor method[J]. Acta Optica Sinica, 2018, 38(2): 0216002.

[34] Li X N, Li Z J, He W T, et al. Enhanced electrochromic properties of nanostructured WO_3 film by combination of chemical and physical methods[J]. Coatings, 2021, 11(8): 959.

[35] Bhattacharjee S, Sen S, Samanta S, et al. Study on the role of rGO in enhancing the electrochromic performance of WO_3 film [J]. Electrochimica Acta, 2022, 427: 140820.

Design and Fabrication of New Curtain-Like WO_3-Based Electrochromic Color-Changing Devices

Chen Guoxin[1], Chen Haoyuan[1], Zhang Zhiyong[1], Zhang Chenchen[1], Tang Xiufeng[1,2*], Zhan Yunfeng[1,2**], Luo Jianyi[1,2***]

[1]*School of Applied Physics and Materials, Wuyi University, Jiangmen* 529020, *Guangdong, China*;

[2]*Research Center of Flexible Sensing Materials and Devices, Wuyi University, Jiangmen* 529020, *Guangdong, China*

Abstract

Objective Electrochromic technology has been widely applied due to its advantages of energy conservation, environmental friendliness, intelligence, and controllability, among which the industrialization of WO_3-based electrochromic devices is most mature. However, in a conventional electrochromic device consisting of upper transparent electrode ITO/counter-electrode/electrolyte/WO_3/lower transparent electrode ITO, the existence of counter-electrode layers not only reduces the transmittance of the device in the bleached state but also affects its cyclic stability due to incomplete matching of the electrochemical properties between the counter-electrode layers and electrochromic layers. Though the structures of electrochromic devices have been continuously optimized, the existing counter-electrode in WO_3-based electrochromic devices cannot be solved. Therefore, this paper first prepares WO_3 films by magnetron sputtering and then fabricates a brand-new curtain-like electrochromic device without a counter-electrode layer based on the "current-driven model". Highly controllable color changes are achieved in the curtain-like device, and influence of the counter-electrode on device performance is eliminated because the counter-electrode is no longer required. This research can provide new pathways for structure innovation of electrochromic devices.

Methods WO_3 films are fabricated by magnetron sputtering of reactive radio frequency (RF) using a W target (purity of 99.99%), an Ar flow rate of 12 sccm (1 sccm=1 m^3/min), and an O_2 flow rate of 4.8 sccm. The substrates are clean ITO glasses with the sheet resistance of 8 Ω/sq. The employed RF power is 80 W, and the substrate heating temperature is 200 ℃. WO_3 films at different thicknesses are obtained through different sputtering durations. Meanwhile, a 1 mol/L Li ion electrolyte is prepared by dissolving $LiClO_4$ in polycarbonate (PC) solution. Finally, the curtain-like WO_3-based electrochromic devices are fabricated by sealing the ITO glass, electrolyte, and WO_3 film with the UV sealant. Scanned electron microscopy images of the WO_3 films are taken on a Sigma 500 instrument (Zeiss) at 10.0 kV. Phase structures of the films and ITO substrate are examined by X-ray diffraction (XRD) analysis through Cu Ka radiation (Philips X′ Pert diffractometer), and X-ray photoelectron spectra (XPS) are recorded by a Thermo Fisher Scientific ESCALAB 250Xi XPS system. Finally, cyclic voltammetry (CV) tests are carried out at the voltage range of −0.8–0.8 V at a scan rate of 100 mV/s on the electrochemical workstation (CHI760E), and transmittance spectra are recorded via the UV-Vis spectrophotometer (Hitachi F-4600, Japan).

Results and Discussions Firstly, amorphous WO_3 films with the thickness of 800 nm are prepared (Fig. 1) and are preferred for ion injection and extraction. The optical modulation rate at wavelength of 550 nm is as high as 78%, and decay rate of the storage charge density is only 3.5% after 1000 CV cycles, which is far better than reported (Fig. 2). Then, curtain-like WO_3-based electrochromic devices are proposed to switch between being colored and bleached without a counter-electrode under the control of a flowing current in the bottom ITO layer (Fig. 3). Bezel between the storage area and the window area of the curtain-like device is designed by introducing an artificial fissure (Fig. 4). Additionally, effect of the WO_3 film thickness on the response time, recovery time and cyclic performances of the device is investigated, and the results show that the best overall performances are realized at film thickness of 800 nm (Fig. 5). The size of the storage area is also explored, and when it is similar with that of the window area, the cyclic performances could be ensured (Fig. 6). Finally, the curtain-like WO_3-based electrochromic device fabricated using the above-mentioned parameters shows a higher transmittance than conventional structured ones, with excellent memory effects (Fig. 7).

Conclusions This paper prepares high-performance WO_3 films by magnetron sputtering, whose modulation rate at a wavelength of 550 nm is as high as 78%, and decay rate of the storage charge density is only 3.5% after 1000 CV cycles. Then a curtain-like electrochromic device without a counter-electrode layer is designed based on the current-driven model, where the bezel, thickness of WO_3 films, and size of the ion storage area are systematically optimized. Results show that an artificially-introduced fissure in the WO_3 film can simultaneously increase the response time and modulation rate of the

device, and facilitates the design of the working area bezel. The overall performances of the device are best when the WO_3 film is at a thickness of 800 nm. The cycling life of the device can be guaranteed when the ion storage area and the working area are similar. Finally, with the employment of optimal designing parameters, the fabricated curtain-like WO_3-based electrochromic device shows excellent performances, and the transparent transmittance at a wavelength of 550 nm is 76%, which is 9 percentage points higher than that of the conventional device with an 80 nm TiO_2 film as the counter-electrode. Moreover, the device also shows an excellent memory effect with the colored transmittance at 20%, only increasing by 7.5 percentage points after being placed for 10 days. These characteristics result in the great application advantages of curtain-like devices in information encryption and famous painting protection. Compared with traditional structures, the curtain-like electrochromic device features a simple structure and highly controllable color-changing patterns, which can provide guidance for the structure innovation of electrochromic devices.

Key words thin films; tungsten oxide; electrochromism; curtain-like; structure simplification